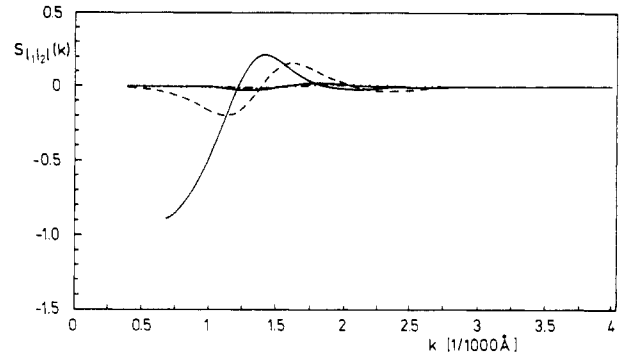

Figure 4. Components of $S(k)$ as defined in (A.6) for L/r_{max} = 0.95. $S_{000}(k)$ solid line), $S_{202} + S_{022}$ (dashed line), S_{220} (dashed-dotted line), S_{222} (dotted line), and S_{224} (solid line with $S_{224}(0) = 0$).

Of particular interest is the contribution of the term with $l = l_1 = l_2 = 0$ to $S(k)$, since it is related to the Fourier transform of the averaged distribution function $\bar{g}(r)$

$$S_{000}(k) = \frac{a_0^2(kL)}{F(k)} \rho \int d^3r \, e^{i\mathbf{k}\cdot\mathbf{r}}(\bar{g}(r) - 1) \qquad (A.8)$$

For small L with $kL < 1$, all $a_l(kL)$ for $l > 0$ are much smaller than $a_0(kL)$. In this case, the sum in (A.5) can be well approximated by its first term (A.8), and by using (A.7) for the form factor, (A.5) reduces to eq 6.

If $kL < 10$, it is sufficient to consider a_0 and a_2 only, since all other a_l are still small. In this case, the structure factor is approximately given by

$$S(k) = 1 + S_{000}(k) + 2S_{202}(k) + S_{220}(k) + S_{222}(k) + S_{224}(k) \qquad (A.9)$$

$S_{202}(k)$ is counted twice, since $S_{022} = S_{202}$. The components used in (A.9) to calculate $S(k)$ are shown in Figure 4 for $L/r_{max} = 0.95$. For all values of L considered, $k_{max}L$ is smaller than 10 and the components S_{220}, S_{222}, and S_{224} are found to be small. Therefore (A.9) is sufficient to calculate $S(k)$ for these values of L/r_{max}.

References and Notes

(1) Hansen, J. P.; Hayter, J. B. *Mol. Phys.* **1982**, *46*, 651. Hayter, J. B.; Penfold, J. *Mol. Phys.* **1981**, *42*, 109.
(2) van Megen, W.; Snook, J. *J. Chem. Phys.* **1977**, *66*, 813.
(3) Hoffmann, H.; Kalus, J.; Thurn, H.; Ibel, K. *Ber. Bunsenges. Phys. Chem.* **1983**, *87*, 1120.
(4) Drifford, M.; Dalbiez, J. P. *J. Phys. Chem.* **1984**, *88*, 5368.
(5) Schneider, J.; Hess, W.; Klein, R. *J. Phys. A* **1985**, *18*, 1221.
(6) Benmouna, M.; Weill, G.; Renoit, H.; Akcasu, A. Z. *J. Phys. (Paris)* **1982**, *43*, 1679.
(7) Brenner, S. L.; Parsegian, V. A. *Biophys. J.* **1974**, *14*, 327.
(8) For the application to scattering experiments on growing micelles one has to take into account that the rodlike micelles contain more monomers than spherical ones and therefore the total charge increases with L.
(9) Pecora, R. *J. Chem. Phys.* **1968**, *48*, 4126.
(10) Hansen, J. P.; McDonald, I. R. *Theory of Simple Liquids*; Academic: New York, 1976.
(11) Metropolis, N.; Rosenbluth, A. W.; Rosenbluth, M. N.; Teller, A. H.; Teller, E. *J. Chem. Phys.* **1953**, *21*, 1087.
(12) Street, W. B.; Gubbins, K. E. *Annu. Rev. Phys. Chem.* **1977**, *28*, 373.
(13) Gray, C. G.; Gubbins, K. E. *Theory of Molecular Fluids*; Clarendon: Oxford, 1984.

Analysis of Enthalpy Relaxation in Poly(methyl methacrylate): Effects of Tacticity, Deuteration, and Thermal History

John J. Tribone,* J. M. O'Reilly, and Jehuda Greener

Research Laboratories, Eastman Kodak Company, Rochester, New York 14650.
Received August 19, 1985; Revised Manuscript Received February 21, 1986

ABSTRACT: Precise differential scanning calorimetry measurements were used to assess the enthalpy relaxation behavior of hydrogenous and deuterated poly(methyl methacrylate) (PMMA), in each of the three stereospecific forms. These polymers provide a set of well-characterized materials with a systematic variation in structure with which the multiorder parameter model can be tested. Materials are held for various times at several sub-T_g annealing temperatures, and results are analyzed in the context of the multiorder parameter model of Narayanaswamy, Kovacs, Moynihan, et al., which assumes thermorheological simplicity, a distribution of relaxation times, and structure-dependent relaxation times. Deuteration has little or no effect on the relaxation behavior and tacticity manifests itself mainly in the magnitude of the activation energy, which scales with the glass transition temperature. The apparent activation energy and the parameter used to characterize the distribution of relaxation times are independent of annealing time and annealing temperature. However, the parameter that characterizes the structure dependence of the relaxation times systematically changes with thermal history, which contradicts its original introduction into the model as a material constant. In addition, the discrepancy between experiment and theory suggests that the model becomes less appropriate as the system approaches closer to equilibrium. It is suggested that the model may be improved by changing the form of the relaxation function and/or modifying the simplified way in which the structure dependence of the relaxation times is introduced.

I. Introduction

Over the years there has been a growing interest in the structural relaxation and recovery processes observed in glassy materials of all kinds, including molecular (organic),[1,2,5] inorganic,[3-5] polymeric,[1,2,6-19] and, more recently, metallic glasses.[20-22] The nature of the problem is clearly related to the intrinsic properties of the "ill-condensed", i.e., nonequilibrium, glassy state, as each of the above classes of materials shows remarkably similar structural relaxation behavior despite obvious differences in the chemical moieties and in the nature of the molecular or atomic forces involved.

Structural relaxation is a result of the nonequilibrium nature of the glassy state, which spontaneously evolves toward some equilibrium state (defined by T and P) at a rate that depends on the temperature, the pressure, and

0024-9297/86/2219-1732$01.50/0

the complete thermomechanical history of the glass.[23] This fact has long been recognized,[24] and a large amount of experimental and theoretical work has been aimed at understanding the observed phenomena.

We report here a systematic investigation of structural recovery in a series of polymer glasses using the heat capacity (or enthalpy), measured in a differential scanning calorimeter (DSC), as the structural probe. Previous studies in this and other laboratories[7-14] have shown the DSC technique to be a convenient and sensitive method of characterizing the recovery process in glasses. The experimental measurements were made on poly(methyl methacrylate) (PMMA); this material provides a convenient means of examining the effects of stereoregularity on the recovery behavior, as the (predominantly) isotactic, syndiotactic, and atactic isomers are readily available. Deuterated polymers of each isomer were prepared [for small-angle neutron scattering (SANS) measurements], and they were also included in our calorimetric investigation.

One of the major objectives of this work was to quantitatively assess the phenomenological order parameter model that has been developed independently in several laboratories.[25-27] From a historical point of view, the model is seen as a modern, cross-disciplinary consolidation of extant experimental evidence whose foundation was laid by Narayanaswamy[25] using ideas previously discussed by Tool.[24]

In addition, this study investigated the effects of stereoregularity and deuteration on the enthalpy relaxation parameters. Effects of stereoregularity on physical properties, e.g., glass transition temperature, mean-square end-to-end distance, and viscoelastic properties, are well-known. In studies of deuterated polymers it is usually assumed that deuteration has little or no effect on properties; however, in a preliminary study we found that the specific heat of deuterated polymers is 10–15% higher than that of their protonated counterparts. This difference is probably due to the lower vibrational frequencies of the deuterated species, due to the larger reduced masses. The analysis of FTIR spectra of deuterated samples suggested that the conformational energy levels change with deuteration.[28] For these reasons we also investigated the relaxation behavior of deuterated stereoregular PMMA.

There are a growing number of experimental studies of physical aging in glassy polymers by a variety of techniques. The multiorder parameter model applied to enthalpy recovery was assessed in a series of papers by Hodge and co-workers;[8-11] they do not report the model parameters as explicit functions of the thermal history but rather as averages over all the thermal treatments examined. For several polymers—poly(vinyl acetate), poly(vinyl chloride), polystyrene, and polycarbonate—the authors report good fits to the data; however, they note that for atactic PMMA the uncertainties in the average parameters are twice as large but do not mention whether the parameters change systematically with changes in thermal history. Prest and co-workers[13] have also developed the computational techniques required to test the multiorder parameter model. These authors use a four-parameter fit and find large changes in the parameters x and β (see section II for definition of parameters) as the thermal history is varied for a polystyrene sample, while the activation energy remains independent of annealing conditions. They also determined the activation energy from the cooling rate dependence of the fictive temperature and find a value twice as large as the optimized value; this seems to be a serious discrepancy between experiment and model. Prest et al.[13] also attempted a simultaneous optimization of experiments with different thermal histories; surprisingly, rather than obtaining values that are a simple average of the individually optimized experiments, they observed x and β values less than any of the previous values and a moderate decrease in the activation energy. This procedure represents an unsatisfactory compromise where the overall quality of the fits is reduced. In any case, the suggestion is made that either the distribution of relaxation times is accounted for improperly or that the structure dependence of the relaxation times needs to be introduced in a different way.

While this work was being completed, another paper appeared on the enthalpy recovery of the three PMMA stereoisomers;[29] the quoted results are brief, and no attempt was made to account for the known nonexponentiality and nonlinearity of the recovery process. Qualitatively, the apparent relaxation time was noted to be larger in isotactic than in atactic and syndiotactic samples at equal values of $(T_g - T_{ann})$.

A number of recent theories[30-36] have provided insight into the complicated many-body behavior of real glasses, and it remains to be seen which approach proves most useful. For this work we have developed the computational and experimental ability to thoroughly check the multiorder parameter model; we review some of the details of this model below.

II. Theory

The order parameter concept as applied to glasses is phenomenological and is based on ideas originally proposed by Davies and Jones;[37] there have been several recent extensions and elaborations of the original theory.[38,39] The point of view of interest in this work was developed independently by Kovacs and co-workers[27] and by Moynihan and co-workers,[26] both groups following earlier ideas of Narayanaswamy[25] and Tool.[24] The model as employed by Kovacs et al.[27] employs a discrete distribution of relaxation times, while Moynihan et al.[26] use a continuous relaxation function; this represents a computational and not a conceptual difference since Kovacs et al.[27] have shown the striking similarity between the continuous distribution and the one derived from the discrete spectrum. The fundamental postulates of the model are that a wide distribution of relaxation times exists (hence the name multiorder parameter model) and that the relaxation times depend on the overall instantaneous structure as well as on T and P. These postulates are well founded experimentally.

The multiorder parameter model is most easily visualized in the context of the classic temperature-jump (T-jump) experiment; the DSC experiment (continuous heating/cooling) is then thought of as a series of infinitesimal T-jumps. In using this formalism it is useful to introduce the concept of the fictive temperature T_f, first introduced by Tool.[24] The fictive temperature represents the relaxing part of the enthalpy (or volume) and is related to the departure of the enthalpy from its equilibrium value as follows:

$$T_f(t) = T + [H(t) - H(\infty)]/\Delta C_p \quad (1)$$

where $H(t)$ and $H(\infty)$ are the enthalpy at time t and at equilibrium ($t = \infty$), respectively, and $\Delta C_p = C_{p,l} - C_{p,g}$, the change in the heat capacity at the glass transition temperature (l denotes liquid; g denotes glass). One can write a general equation for any relaxing quantity, which has the following form:

$$T_f(t) = T_0 + \Delta T[1 - \phi(t)] \quad (2)$$

where T_0 is the initial temperature at which equilibrium

Table I
Molecular Weights and Glass Transition Temperatures of PMMA Samples

	$\bar{M}_w \times 10^{-3}$ [a]		T_g [b]	
	H	D	H	D
isotactic	120	109	326	326
syndiotactic	72	62	396	395
atactic	104	101	376[c]	388[c]

[a] Determined by light scattering. [b] Defined at the onset of the glass transition region on heating at 20 °C/min for unannealed samples. [c] The difference in T_g between the H and D polymers is thought to be due to the low value of T_g of the H polymer. The exact cause of the low value is not known but the relaxation parameters are apparently not affected by this difference.

has been established, ΔT is the magnitude of the temperature jump, and $\phi(t)$ is the relaxation function. The relaxation function must account for four major experimental observations: (1) nonexponentiality, i.e., $d \ln \phi(t)/dt \neq$ constant, (2) nonlinearity, i.e., $\phi(t)$ depends on the magnitude of the T-jump, (3) asymmetry, i.e., $\phi(t)$ depends on the direction of the T-jump, and (4) memory effects that are observed in multiple T-jump experiments.

The most widely used relaxation function is the empirical Williams–Watts function,[40] generalized to the nonlinear case

$$\phi(t) = \exp\left\{-\left[\int_0^t dt'/\tau(t)\right]^\beta\right\} \quad (3)$$

where β ($0 < \beta \leq 1$) is a parameter that characterizes the width of the distribution of relaxation times and τ is a characteristic time that depends on both the actual temperature and the fictive temperature, i.e., on the instantaneous state of the glass.

Several relations have been proposed for τ, but Kovacs et al.[41] have shown that they can all be written as originally proposed by Narayanaswamy[25]

$$\tau(T,T_f) = A \exp[(x\Delta h/RT) + (1 - x)\Delta h/RT_f] \quad (4)$$

where A is the relaxation time at some arbitrary reference temperature, Δh is an activation enthalpy, and x is an empirical parameter introduced by Narayanaswamy[25] that partitions the temperature and structure dependence of τ. Introducing eq 3 into eq 2, transforming from t to T using $q = dT/dt$, and summing over all the instantaneous T-jumps, one finally obtains

$$T_f(t) = T_0 + \int_{T_0}^{T} dT'\left[1 - \exp\left\{-\left[\int_{T'}^{T} dT''/q\tau(T,T_f)\right]^\beta\right\}\right] \quad (5)$$

where T' and T'' are dummy integration variables. This is the working equation of the model for the case of continuous heating and cooling; the attractive feature of the model is that it can accept any thermal history provided the initial state is known, which in practice means starting from equilibrium ($T = T_f$). However, it is implicit in T_f [since $\tau = \tau(T,T_f)$] and must be solved by numerical methods, which will be outlined below.

III. Experiments and Analysis

The samples were obtained from previous work.[28,42] Table I lists the molecular weights determined from light scattering and the glass transition temperatures from DSC.

Details of the computer-interfaced calorimeter are given elsewhere;[43] the precision of this instrument for measuring heat capacities of polymers is 1–2%.

All the experiments reported here were run at fixed heating and cooling rates of 20 °C/min, and data were collected only on heating. Figure 1 shows the thermal histories of materials used in these experiments. In a typical experiment, the sample is first equilibrated at a temperature (T_H) well above the glass transition region and then cooled at the chosen rate to a temperature (T_L) well below T_g where aging effects are minimal on the experimental time scale. After a short holding period (kept constant in these experiments), the sample is heated at the desired rate through the glass transition region; this history is designated "unannealed". During the next cycle, instead of being cooled directly to T_L, the sample is held at a desired sub-T_g temperature (T_{ann}) for a certain time (t_{ann}) before it is cooled again to the low temperature; therefore, on heating in the next cycle the sample has a known thermal history, which is reflected in the well-known overshoot phenomenon at the glass transition. In this work the annealing temperatures were kept in the range T_g – 25 °C to T_g and annealing times in the range 0–1000 min.

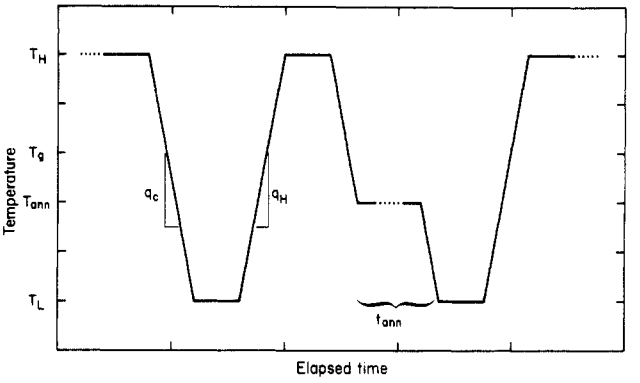

Figure 1. Schematic thermal history in a DSC annealing experiment.

The fictive temperature is obtained from eq 5, which is an implicit integral equation of the Volterra type. This equation is solved by an explicit iterative scheme, wherein the double integral is evaluated by the trapezoidal rule. To ensure convergence during a given step, the calculated value of T_f must agree with the value of the previous iteration to within an amount ϵ, where ϵ is typically taken to be 0.01. During the cooling and heating phases in a typical computational cycle, the temperature is stepped by 0.1 °C or less, whereas during annealing the time is divided into several (usually 10) equal logarithmic intervals. The numerical scheme usually converges rapidly, requiring a small number (<3) of iterations. The parameters in eq 4 and 5 are estimated by use of a modified Gauss–Newton optimization routine. In this analysis we chose to fix A and optimize on x, β, and Δh, using data of dT_f/dT vs. T. Depending on the general features of the response function and particularly on the height of the annealing peak, the number of iterations in the optimization scheme could vary in the range 5–50. The standard error in the optimization fit is usually <0.1. Prest and co-workers[13] have shown, not surprisingly, that a four-parameter optimization improves the fit to the data, although the general trends of the solution are qualitatively the same.

The apparent activation energy Δh can be estimated independently from the heating or cooling rate (q_H or q_C) dependence of the limiting fictive temperature (T_f') or, equivalently, the glass transition temperature as it is usually defined[26b]

$$\Delta h \simeq -R[d \ln q/d(1/T_f')] \simeq -R[d \ln q/d(1/T_g)] \quad (6)$$

where R is the gas constant. The derivation of eq 6 is

Table II
Temperature Dependence of the Heat Capacity and the Change in C_p at T_g

sample[a]	T_g, K	T_{ann}, K	$dC_{p,l}/dT$	$dC_{p,g}/dT$	$d\Delta C_p/dT$	$\Delta C_p(T_g)$
I-PMMA	326	305	0.0032	0.0055	−0.0023	0.367
		319	0.0026	0.0069	−0.0042	0.382
D-I-PMMA	326	305	0.0028	0.0069	−0.0041	0.364
		319	0.0026	0.0068	−0.0042	0.372
A-PMMA	376	362	0.0029	0.0059	−0.0030	0.293
		370	0.0031	0.0054	−0.0023	0.292
D-A-PMMA	388	370	0.0042	0.0052	−0.0010	0.297
		381	0.0041	0.0050	−0.0009	0.258
S-PMMA	396	380	0.0033	0.0045	−0.0012	0.306
		389	0.0037	0.0048	−0.0011	0.276
D-S-PMMA	395	380	0.0034	0.0045	−0.0011	0.283
		389	0.0033	0.0049	−0.0016	0.260

[a] I = isotactic, A = atactic, S = syndiotactic, and D = deuterated.

strictly based on the case where $q_C = -q_H$; however, independent experiments[44] have shown that the activation energy does not differ greatly between the case where $q_C = -q_H$ on the one hand and the case where the cooling rate is kept constant at 20 °C/min on the other. This is probably because of the small range of rates available practically. Therefore, the present determination of Δh is based on experiments where q_C was fixed at 20 °C/min. Initial estimates of Δh for use in the optimization program (see below) are obtained in this way. Furthermore, if one assumes that the value of the average relaxation time at $T_g[\tau(T_g)]$ is nearly constant for various materials, then Δh and ln A are not independent parameters

$$\ln A \simeq \ln \tau(T_g) - \Delta h/RT_g \quad (7)$$

which follows from eq 4 if $T_f \simeq T$ at T_g. Estimates of ln A are obtained in this self-consistent way.

IV. Results

A. Model Calculations. To give a qualitative sense of the effect of the parameters on the calculated recovery curves, some sample calculations are illustrated in Figure 2; the parameters are given in the figure. For small values of β (Figure 2A) the recovery curve is smeared out over a wide temperature range, and a shallow peak develops at temperatures below the normal T_g peak; this peak shifts to lower temperatures as x increases. At intermediate values of β (Figure 2B) recovery is very sensitive to x for small x, with the peak shifting to higher temperature as x decreases; at larger values of x, recovery is less sensitive to variations in x. Finally, at large β (Figure 2C), the recovery curves are very sensitive to changes in x over the full range of x; again, the peak shifts to higher temperature as x decreases.

B. DSC Results. Typical experimental results for each of the stereoisomers are shown in Figure 3; these three plots are for annealing at temperatures roughly the same distance from T_g, i.e., $(T_g - T_{ann}) \simeq$ constant $\simeq$ 15 K, so that the relative annealing characteristics can be compared directly (note, however, the differences in ΔC_p). These curves can be converted directly into dT_f/dT through eq 1 by using the experimental $C_{p,l}$ and $C_{p,g}$.

Table II lists the measured temperature dependence of $C_{p,l}$, $C_{p,g}$, and the change in C_p at the glass transition for each sample at various annnealing temperatures. The slopes are obtained by a least-squares fit to a linear equation of the form $C_p = a + bT$.

Figure 4 compares a few experimental and calculated curves; the examples are typical of the general trends in the results. Each curve representing a given annealing time and temperature is fit to the model individually by using the aforementioned optimization routine. In all the cases examined so far, the calculated curves are reasonably good

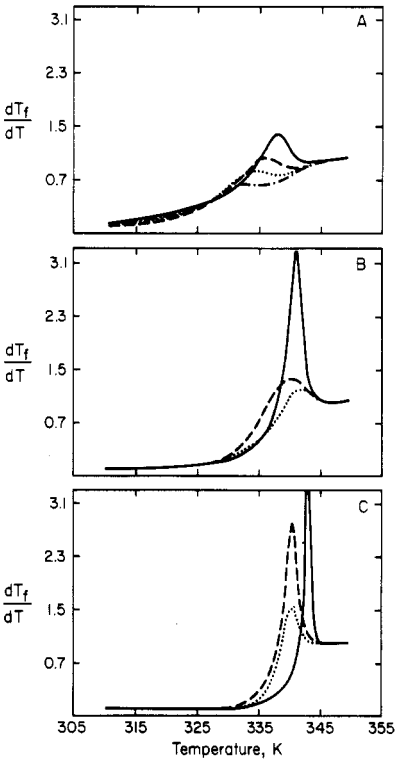

Figure 2. Calculated enthalpy recovery curves with the following parameters: ln A = 235, T_H 350 K, T_{ann} = 320 K, T_L = 310 K, $q_H = -q_C$ = 20 °C/min, t_{ann} = 18 000 s. (A) β = 0.2; x = 0.2 (–), 0.4 (– – –), 0.6 (···), 0.8 (–·–). (B) β = 0.5; x = 0.4 (—), 0.6 (– – –), 0.8 (···). (C) β = 0.8; x = 0.4 (—), 0.6 (– – –), 0.8 (···). Plotted as normalized heat capacity: $dT_f/dT \equiv [C_p(T) - C_{p,g}(T)]/[C_{p,l}(T) - C_{p,g}(T)]$ (l = liquid, g = glass).

approximations to the experimental data; the model predicts the position and the height of the peak rather well but fails to mimic the detailed shape of the experimental curves, especially when the system is near equilibrium. Allowing the fourth parameter, ln A, to be included in the optimization will improve this situation considerably but will not change the major conclusions of this study; in fact, the shortcomings of the model discussed below are only magnified by permitting the fourth parameter to float in the optimization.

In the following figures the effect of thermal history on the model parameters (x, β, and Δh) is shown. Figure 5 shows representative results for isotactic PMMA annealed at 295 K; x changes linearly with annealing time and β and Δh are nearly independent of annealing time. Figure 5 also shows that, within experimental error, the effect of deuteration on the relaxation parameters is negligible; this is true for all the samples studied. The heat capacities of

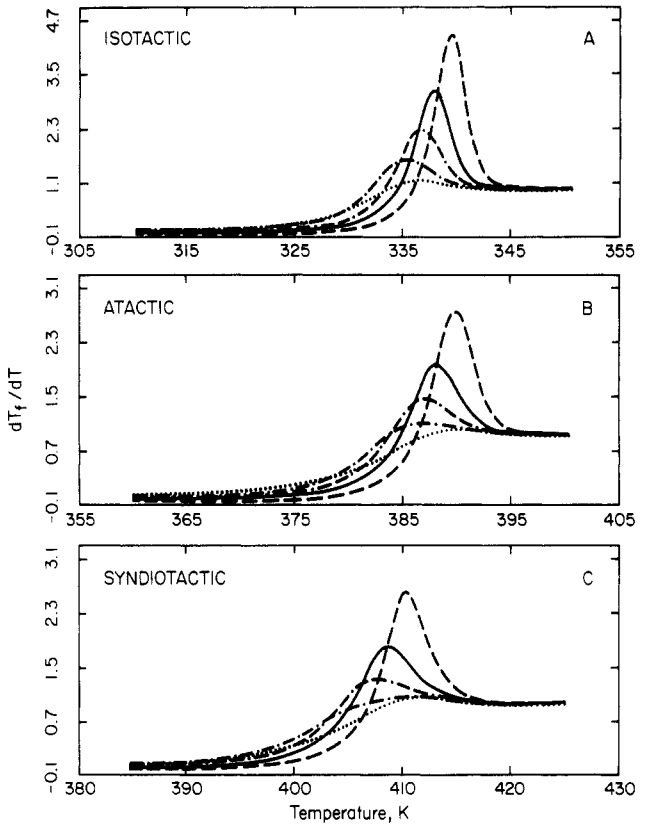

Figure 3. Experimental enthalpy recovery curves; t_{ann} = 0 s (···), 1800 s (-·-), 6000 s (·---·), 18000 s (—), 60000 s (---). (A) Isotactic PMMA, T_{ann} = 311 K. (B) Atactic PMMA, T_{ann} = 362 K. (C) Syndiotactic PMMA, T_{ann} = 380 K. Annealing temperatures are all approximately 15 K below the respective T_g's.

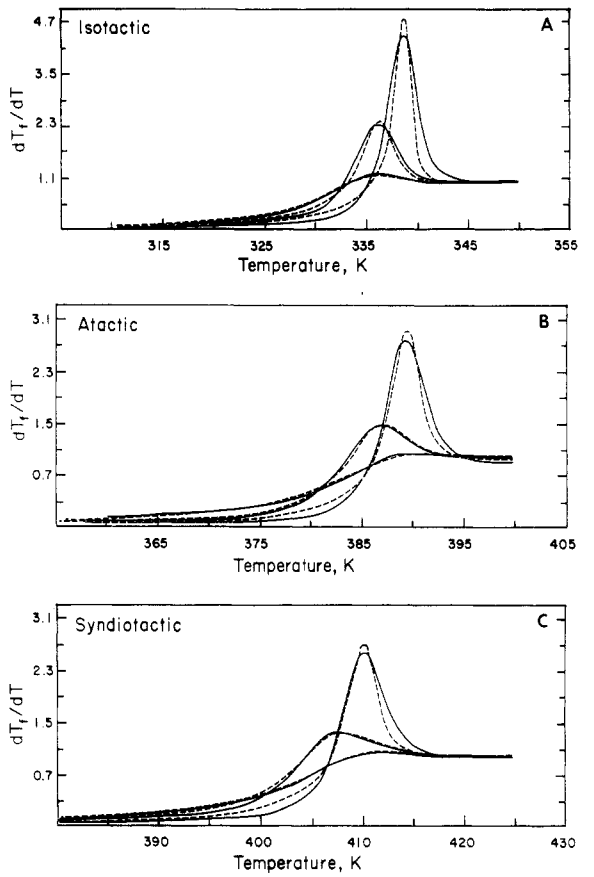

Figure 4. Comparison of experimental (solid) and calculated (dashed) enthalpy recovery curves. (A), (B), and (C) same as in Figure 3. The curves represent t_{ann} = 0, 6000, and 60000 s, peak height increasing with increasing annealing time.

the deuterated polymers are 10–15% higher than those of the hydrogenous polymers. This difference is attributed to the lower vibrational frequencies of the deuterated materials. One would not expect to see large differences in glassy structure and dynamics with deuteration, and this is borne out by the experiments. Instead the excellent agreement between deuterated and hydrogenous PMMA shows the reproducibility and consistency of the measurements and analysis.

In some cases the parameters obtained for the unannealed samples do not follow the same trend as the annealed samples; this is true even though the model can predict these curves very accurately, owing to their relatively simple shape. It is not clear whether this represents an artifact of the analysis or is an intrinsic deficiency of the model; in rare instances this is not observed, which suggests that the effect is real. In any case, data points corresponding to unannealed samples were not included in any of the comparisons.

Each sample was also been annealed at several different temperatures below T_g. Figure 6, parts A and B, shows the variation in x and β at two different annealing temperatures for each stereoisomer. It is clear that x depends significantly on annealing temperature, increasing as the annealing temperature increases. The distribution parameter is insensitive to annealing temperature, and all the results fall in a narrow band around β = 0.4. The annealing temperature has little effect on the slope of these curves.

We saw in Figure 5 that the activation energy is independent of annealing time. These experiments also show that the activation energy is independent of annealing temperature (Figure 6C). However, Δh is very sensitive

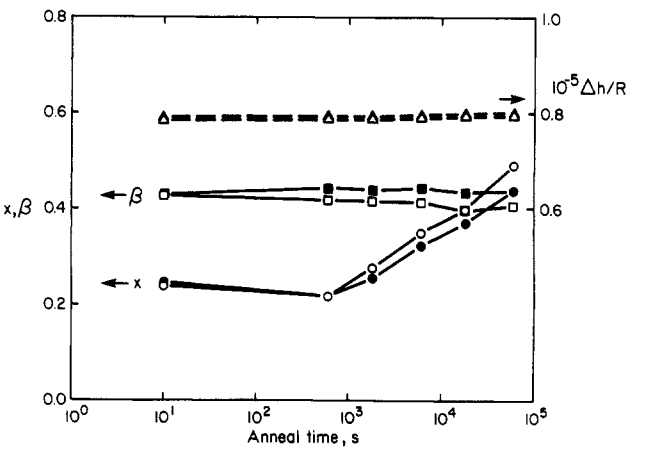

Figure 5. Variation of x, β, and $\Delta h/R$ with annealing time for isotactic PMMA annealed at 319 K. Open symbols, hydrogeneous samples; filled symbols, deuterated samples. Unannealed samples are arbitrarily shown at t_{ann} = 10 s.

Table III
Apparent Activation Energies Estimated from the Heating Rate Dependence of T_g

	Δh,[a] kcal/mol	$\Delta h/T_g$, kcal/(mol·K)
isotactic	160	0.49
atactic	210	0.56
syndiotactic	230	0.58

[a] Δh determined from the heating rate dependence of the glass transition temperature for samples cooled through the transition at a constant rate of 20 °C/min.

to the stereochemistry of these materials and scales directly with the glass transition temperature (Table III).

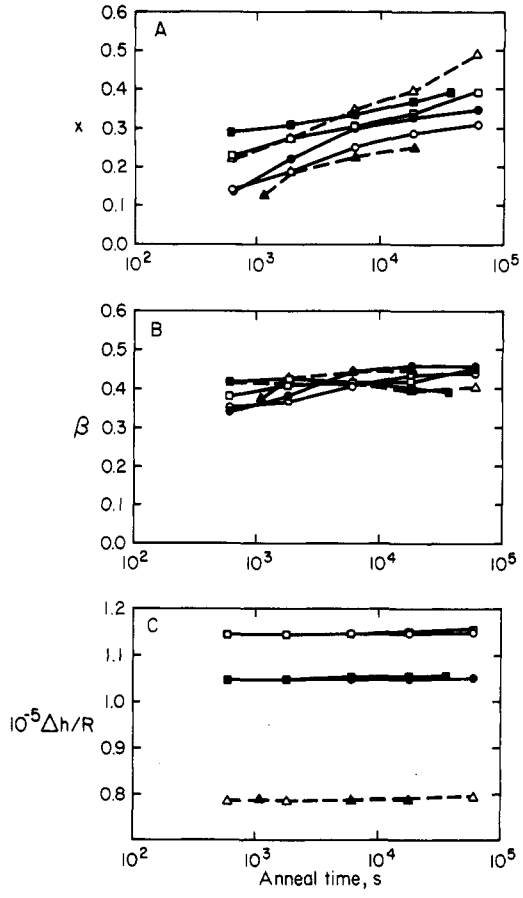

Figure 6. Variation of x, β, and $\Delta h/R$ with annealing time for several hydrogeneous samples: syndiotactic, T_{ann} = 380 K (○), 389 K (□); atactic, T_{ann} = 362 K (●), 370 K (■); isotactic, T_{ann} = 305 K (▲), 319 K (△).

V. Discussion

Acknowledging the inherent flexibility of the multiorder parameter model, we nonetheless maintain that it is crucial to test the model for the simplest thermal histories with precise experimental data provided by computer-controlled DSC. On the other hand, mounting experimental evidence makes it clear that this model can be applied semiquantitatively for almost any thermal or stress history.

Although the model can account convincingly for the experimental recovery curves at short annealing times, it begins to break down quantitatively for long annealing times. In addition, the parameter x is required to be a function of both annealing time and annealing temperature when it is obtained by optimization; this fact cannot be reconciled easily with the original development of the theory, wherein x is not considered to be explicitly dependent on annealing conditions. Empirically allowing the parameters to depend on thermal history would simply add to the number of adjustable parameters but not to the physical insight.

The partitioning parameter x is empirically defined as the fraction of the relaxation time that is due solely to the absolute temperature of the system; its complement, $(1 - x)$, defines that part of the relaxation time that is determined by the instantaneous state of the system as reflected in the fictive temperature. If we follow the original ideas of Tool[24] and assume that an annealing glass explores phase space in such a way as to pass through a series of states that are equivalent to hypothetical equilibrium states at T_f, then one would expect the structural contribution to τ to be independent of thermal history, since structural changes are a result of some fixed path through phase space. However, even Tool himself had doubts about this hypothesis, despite good agreement with limited data at that time.[24] (Empirically, the partitioning of the activation energy according to eq 4 is independent of the way in which the fictive temperature is interpreted physically.) This is not to say that the fictive temperature is not useful as a conceptual measure of the state of the glass, only that its physical interpretation is not well-defined. Therefore it seems that this simplified way of partitioning the relaxation times may be part of the cause of the discrepancy between experiment and theory. This had been suggested by Prest et al.[13]

The second parameter, β, is an empirical measure of the width of the distribution of relaxation times. The model makes an explicit assumption that β is independent of temperature by assuming thermorheological simplicity. It is not surprising that this assumption may break down in light of several other experimental results.[45,46] The present resuls show only minor changes in β with annealing time and temperature, and it is not appropriate to draw detailed conclusions about changes in the relaxation spectrum. Nonetheless, Prest et al.[13] saw much larger changes in β when a four-parameter optimization was used; they also suggest that the Williams–Watts function may be an inadequate representation of the distribution. A large body of data is accurately represented by this function, but when one looks carefully at the short-time portion of the Williams–Watts distribution, some discrepancies appear.[47] However, it is still not clear whether changes in the parameters with thermal history might be eliminated by proper choice of the structure dependence and/or the distribution function. We note that in the Ngai model[31] the distribution parameter is considered an explicit function of both temperature and annealing time.

The third parameter, Δh, represents an average activation energy for structural relaxation. For PMMA it clearly depends on the stereochemistry and hence on T_g. Karasz and MacKnight[48] have related the difference in T_g between isotactic and syndiotactic isomers to the difference in conformational energies of the rotational isomers; the fact that the measured Δh scales directly with T_g suggests that it is related to the conformational energy barrier. However, its magnitude reflects the cooperative nature of the recovery process. The multiorder parameter model assumes that the activation enthalpy is constant and hence that the temperature dependence is Arrhenius. This assumption has not been tested adequately in light of the known non-Arrhenius behavior of amorphous materials in the glass transition region. There are several ways of describing the functional form of the relaxation time: WLF or Vogel–Tammann–Fulcher[49] and Adam–Gibbs,[50] representing free-volume-controlled and configurational-entropy-controlled processes, respectively. Scherer[51] incorporated the Adam–Gibbs formalism into the multiorder parameter model and found good agreement with a limited set of data for a soda-lime silicate glass (NBS 710); nevertheless, significant differences between the Arrhenius and Adam–Gibbs relations show up only at very high cooling rates. Furthermore, strictly following the Adam–Gibbs formalism leads to the conclusion that the relaxation time for any property depends on the fictive temperature for the enthalpy; an ad hoc, but logical, assumption is necessary to generalize the Adam–Gibbs result.

Most of the available data show that the model becomes less accurate as the departure from equilibrium becomes small, i.e., as t_{ann} becomes large and/or T_{ann} approaches T_g. Even though this region will, by definition, have the largest peaks, the results are not consistent with the idea

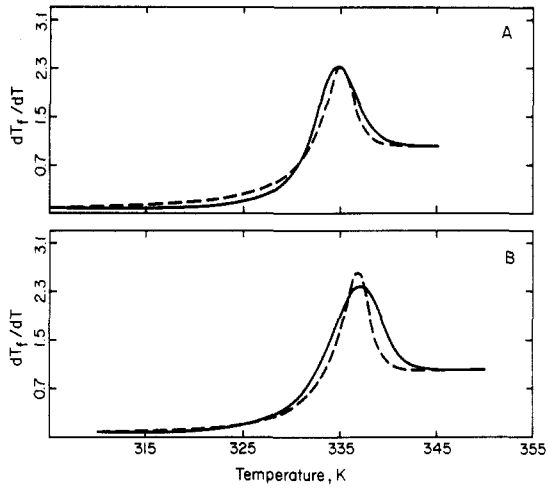

Figure 7. Comparison of experimental (solid) and calculated (dashed) enthalpy recovery curves for isotactic PMMA annealed for 18 000 s. (A) T_{ann} = 305 K, standard error = 0.107; (B) T_{ann} = 319 K, standard error = 0.183.

that it is naturally harder to fit larger and/or sharper peaks than to fit smaller and/or broader ones. Although this is generally a good rule of thumb, the data show that peaks of nearly equal height are fit better or worse depending on the absolute departure from equilibrium, i.e., on the annealing time and the annealing temperature. This is illustrated in Figure 7 for isotactic PMMA annealed for a constant time (18 000 s) at two annealing temperatures; even though the peaks are similar in magnitude the fit is worse at higher T_{ann}, since at this temperature the enthalpy is nearer its equilibrium value. It is clearly not the sharpness of the experimental peaks that limits the quality of fit, since the calculations always predict a narrower peak than is observed.

VI. Summary and Conclusions

We examined the enthalpy relaxation behavior of PMMA as a function of tacticity, deuteration, and thermal history, using a computer-controlled DSC capable of high-precision heat capacity measurements. Results were used to investigate in detail the validity of the phenomenological order-parameter model of glass transition kinetics. The model provides a good quantitative description of the experimental recovery data at short annealing times, but the fits become poorer as the annealing time increases. At constant annealing time, in the long-time region, the fits become worse as the annealing temperature is increased toward the glass transition temperature. In a more general context, the discrepancy between experiment and theory is larger as the enthalpy becomes closer to its equilibrium value. In practice, this means that a large annealing peak observed at low annealing temperatures is able to fit better than the same height peak obtained at higher annealing temperatures (assuming the peak widths are similar).

Furthermore, achieving the best possible coincidence between experiment and theory requires the nonlinearity parameter x to be a function of thermal history; this contradicts the original postulate that x is a material constant. It is thus possible that the way in which the relaxation times are partitioned between temperature and structure is inadequate and/or the assumed fractional exponential distribution function (Williams–Watts) does not give an accurate representation of the underlying physical mechanisms involved in the enthalpy relaxation process.

The effect of deuteration on the relaxation parameters is expectedly negligible, but the consistency of the results between hydrogenous and deuterated samples shows the reproducibility of both the measurements and the analysis.

Tacticity has only a small effect on the parameters x and β but has a pronounced effect on the activation enthalpy, which scales directly with the glass transition temperature. The magnitude of the activation enthalpy (~200 kcal/mol) is indicative of the highly cooperative nature of the recovery process in glasses.

Registry No. Isotactic PMMA, 25188-98-1; isotactic PMMA (deuterated), 79487-31-3; syndiotactic PMMA, 25188-97-0; syndiotactic PMMA (deuterated), 79547-91-4; atactic PMMA, 9011-14-7; atactic PMMA (deuterated), 63541-79-7.

References and Notes

(1) Struik, L. C. E. *Physical Aging of Amorphous Polymers and Other Materials*; Elsevier: New York, 1978.
(2) Marshall, A. S.; Petrie, S. E. B. *J. Appl. Phys.* **1975**, *46*, 4223.
(3) Moynihan, C. T.; Macedo, P. B.; Montrose, C. J.; Gupta, P. K.; Debolt, M. A.; Dill, J. F.; Dom, B. E.; Drake, P. W.; Easteal, A. J.; Elterman, P. B.; Moeller, R. A.; Sasabe, H.; Wilder, J. A. *Ann. N.Y. Acad. Sci.* **1976**, *279*, 15.
(4) Chen, H. S.; Kurkjian, C. R. *J. Am. Ceram. Soc.* **1983**, *66*, 613.
(5) Barkatt, A.; Angell, C. A. *J. Phys. Chem.* **1978**, *82*, 1972; *J. Chem. Phys.* **1979**, *70*, 901.
(6) Kovacs, A. J. *Fortschr. Hochpolym.-Forsch.* **1963**, *3*, 394.
(7) O'Reilly, J. M. In *Structure and Properties of Amorphous Polymers*; Walton, A. G., Ed.; Elsevier: Amsterdam, 1980.
(8) Berens, A. R.; Hodge, I. M. *Macromolecules* **1982**, *15*, 756.
(9) Hodge, I. M.; Berens, A. R. *Macromolecules* **1982**, *15*, 762.
(10) Hodge, I. M.; Huvard, G. S. *Macromolecules* **1983**, *16*, 371.
(11) Hodge, I. M. *Macromolecules* **1983**, *16*, 898.
(12) Prest, W. M., Jr.; Roberts, F. J., Jr. *Ann. N.Y. Acad. Sci.* **1981**, *371*, 67.
(13) Prest, W. M., Jr.; Roberts, F. J., Jr.; Hodge, I. M. *Proc. 12th North Am. Therm. Anal. Soc. Conf.* Sept. 25–29, 1980, Williamsburg, VA, pp 119–123.
(14) Chen, H. S.; Wang, T. T. *J. Appl. Phys.* **1981**, *52*, 5898.
(15) Lamarre, L.; Sung, C. S. P. *Macromolecules* **1983**, *16*, 1729.
(16) Wendorff, J. H. *J. Polym. Sci., Polym. Lett. Ed.* **1979**, *17*, 765.
(17) Roe, R-J.; Curro, J. J. *Macromolecules* **1983**, *16*, 428.
(18) Roe, R-J.; Millman, G. M. *Polym. Eng. Sci.* **1983**, *23*, 318.
(19) Adachi, K.; Kotaka, T. *Polym. J. (Tokyo)* **1982**, *14*, 959.
(20) Chen, H. S. *J. Appl. Phys.* **1981**, *52*, 1868.
(21) Greer, A. L.; Spaepen, F. *Ann. N.Y. Acad. Sci.* **1981**, *371*, 218.
(22) Egami, T. *Ann. N.Y. Acad. Sci.* **1981**, *371*, 238.
(23) Kovacs, A. J. *Ann. N.Y. Acad. Sci.* **1981**, *371*, 38.
(24) Tool, A. Q. *J. Am. Ceram. Soc.* **1946**, *29*, 240.
(25) Narayanaswamy, O. S. *J. Am. Ceram. Soc.* **1971**, *54*, 491.
(26) (a) Debolt, M. A.; Easteal, A. J.; Macedo, P. B.; Moynihan, C. T. *J. Am. Ceram. Soc.* **1976**, *59*, 16. (b) Moynihan, C. T.; Easteal, A. J.; Debolt, M. A. *J. Am. Ceram. Soc.* **1976**, *59*, 12.
(27) Kovacs, A. J.; Aklonis, J. J.; Hutchinson, J. M.; Ramos, A. R. *J. Polym. Sci., Polym. Phys. Ed.* **1979**, *17*, 1097.
(28) O'Reilly, J. M.; Mosher, R. A. *Macromolecules* **1981**, *14*, 602. O'Reilly, J. M.; Teegarden, D. M.; Mosher, R. A. *Macromolecules* **1981**, *14*, 1693.
(29) Yoshida, H.; Kobayashi, Y. *Polym. J. (Tokyo)* **1982**, *14*, 925.
(30) (a) Robertson, R. E. *J. Polym. Sci., Polym. Symp.* **1978**, *No. 63*, 173; *Ann. N.Y. Acad. Sci.* **1981**, *371*, 21. (b) Robertson, R. E.; Simha, R.; Curro, J. G. *Macromolecules* **1984**, *17*, 911. (c) Simha, R.; Curro, J. G.; Robertson, R. E. *Polym. Eng. Sci.* **1984**, *24*, 1071.
(31) Ngai, K. L. *Comments Solid State Phys.* **1979**, *9*, 127; *J. Phys., Colloq.* **1982**, *C9 43*, 607.
(32) Rendell, R. W.; Lee, T. K.; Ngai, K. L. *Polym. Eng. Sci.* **1984**, *24*, 1104.
(33) Hill, R. M.; Jonscher, A. K. *Contemp. Phys.* **1983**, *24*, 75.
(34) Balik, C. M.; Jamieson, A. M.; Simha, R. *Colloid Polym. Sci.* **1982**, *260*, 477. Simha, R.; Jain, S. C.; Jamieson, A. M. *Macromolecules* **1982**, *15*, 1517, 1522.
(35) Curro, J. G.; Lagasse, R. R.; Simha, R. *Macromolecules* **1982**, *15*, 1621.
(36) Chow, T. S. *J. Chem. Phys.* **1983**, *79*, 4602; *J. Polym. Sci., Polym. Phys. Ed.* **1984**, *22*, 699; *Polym. Eng. Sci.* **1984**, *24*, 1079.
(37) Davies, R. O.; Jones, G. O. *Adv. Phys.* **1953**, *2*, 370; *Proc. R. Soc. London, A* **1953**, *217*, 26.
(38) Roe, R-J. *J. Appl. Phys.* **1977**, *48*, 4085.
(39) Berg, J. I.; Cooper, A. R. *J. Chem. Phys.* **1978**, *68*, 4481.

(40) (a) Williams, G.; Watts, D. C. *Trans. Faraday Soc.* **1970**, *66*, 80. (b) Shlesinger, M. F.; Montroll, E. W. *Proc. Natl. Acad. Sci. U.S.A.* **1984**, *81*, 1280.
(41) Kovacs, A. J.; Hutchinson, J. M.; Aklonis, J. J. In *The Structure of Non-Crystalline Materials*; Gaskell, P. H., Ed.; Taylor and Francis: London, 1977.
(42) O'Reilly, J. M.; Bair, H. E.; Karasz, F. E. *Macromolecules* **1982**, *15*, 1083.
(43) O'Reilly, J. M.; Connelly, R. *Thermochim. Acta* **1985**, *86*, 231.
(44) Tribone, J. J., unpublished results.
(45) Plazek, D. J.; Ngai, K. L.; Rendell, R. W. *Polym. Eng. Sci.* **1984**, *24*, 1111.
(46) McCrum, N. G. *Polym. Commun.* **1984**, *25*, 2; *Polymer* **1984**, *25*, 309.
(47) Brawer, S. A. *J. Chem. Phys.* **1984**, *81*, 954.
(48) Karasz, F. E.; MacKnight, W. J. *Macromolecules* **1968**, *1*, 537.
(49) (a) Williams, M. L.; Landel, R. F.; Ferry, J. D. *J. Am. Chem. Soc.* **1955**, *77*, 3701. (b) Vogel, H. *Phys. Z.* **1921**, *22*, 645. Fulcher, G. S. *J. Am. Ceram. Soc.* **1925**, *8*, 339. Tammann, G.; Hesse, G. *Z. Anorg. Allg. Chem.* **1926**, *156*, 245. (c) Angell, C. A.; Smith, D. L. *J. Phys. Chem.* **1982**, *86*, 3845.
(50) Adam, G.; Gibbs, J. H. *J. Chem. Phys.* **1965**, *43*, 139.
(51) Scherer, G. W. *J. Am. Ceram. Soc.* **1984**, *67*, 504.

Effect of Finite Chain Length on the Helix/Coil Coexistence Behavior of Polymers: Poly(oxymethylene)†

J. G. Curro,* K. S. Schweizer, and D. Adolf

Sandia National Laboratories, Albuquerque, New Mexico 87185

James E. Mark

Department of Chemistry, University of Cincinnati, Cincinnati, Ohio 45221.
Received December 31, 1985

ABSTRACT: Monte Carlo calculations were performed on poly(oxymethylene) chains using the rotational isomeric state model. The end-to-end distribution function was found to exhibit bimodal behavior, characteristic of a helix/coil coexistence, over a range of temperature and chain length. The first-order gauche distribution (P_G) and the second-order gauche pair distribution (P_{GG}) did not show any bimodality. The sequence length distribution, however, did show pronounced bimodality. The transition-like behavior was found to become sharper and shifts to lower temperature with a logarithmic dependence on the chain length. Thus the helix/coil coexistence behavior is a finite chain effect, with the transition temperature approaching 0 K for the infinite system. As expected, an external force on the ends of the chain was found to shift the coexistence temperature to higher temperatures. These results can be understood by analogy with the one-dimensional Ising model.

Introduction

Poly(oxymethylene) (POM) is an interesting polymer because it is an example of a synthetic chain in which the gauche state has a significantly lower energy than the trans state. This energy difference, which is thought to be due to attractive interactions between CH_2 and O groups, is estimated to be −1.4 kcal/mol on the basis of semiempirical conformational energy calculations and dipole moment measurements.[1-4] The preference for gauche configurations, coupled with severe repulsive interactions for alternate gauche bonds of opposite sign, gives POM a strong tendency to form helical sequences.[1]

Distribution functions for POM chains were computed previously[5] from Monte Carlo simulations for rotational isomeric state chains. The tendency toward helix formation was manifested by a curious bimodal shape for the end-to-end distribution function. This "bimodality", which increases as the temperature is lowered, is suggestive of a helix/coil transition. Such a phenomenon cannot be a true phase transition, of course, since the rotational isomeric state model is a one-dimensional, Ising-like model,[6] for which no thermodynamic phase transition can exist at finite temperature. Rather it is a pseudo-first-order coexistence behavior which occurs due to finite size effects.

The purpose of the present investigation is to examine the configurational statistics of POM in more detail in order to gain a further understanding of this helix/coil coexistence behavior observed in the end-to-end distribution function. In addition, we have computed various internal sequence distributions for POM from computer simulations of rotational isomeric state chains. We also examine the influence of an external field on the end-to-end distribution function. In a broader context, the present study is representative of the variety of physical behavior that can occur in polymer chains of moderate length.

Monte Carlo Simulations

The Monte Carlo scheme here uses a modified Metropolis[7] algorithm to compute the average $\langle X \rangle$ of some observable variable X_i which depends on the chain configuration.[8] $\{\phi\}_i$ represents the set $\{\phi_1 \ldots \phi_N\}_i$ of possible rotational states (t, g^+, g^-) for a specific chain i of N repeat units. For a canonical ensemble, $\langle X \rangle$ takes the form

$$\langle X \rangle = \sum_i X_i \Omega_i / \sum_i \Omega_i \qquad (1)$$

where the subscript refers to a specific set of many possible configurations $\{\phi\}_i$. The coefficient Ω_i is the Boltzmann factor for the configuration i.

Using the conventional rotational isomeric state[1] formalism for POM, we can define two statistical weight matrices for a pair of bonds.

$$\mathbf{U}_a = \begin{pmatrix} 1 & \sigma & \sigma \\ 1 & \sigma & \sigma\omega_a \\ 1 & \sigma\omega_a & \sigma \end{pmatrix} \qquad (2a)$$

$$\mathbf{U}_b = \begin{pmatrix} 1 & \sigma & \sigma \\ 1 & \sigma & \sigma\omega_b \\ 1 & \sigma\omega_b & \sigma \end{pmatrix} \qquad (2b)$$

† Supported by the U.S. Department of Energy under Contract No. DE-AC04-76DP00789 and the National Science Foundation (J.E.M.) through Grant DMR79-18903-03 (Polymers Program, Division of Materials Research).

0024-9297/86/2219-1739$01.50/0